2019 International Conference on Robotics and Automation (ICRA)
Palais des congres de Montreal, Montreal, Canada, May 20-24, 2019

Workspace CPG with Body Pose Control for Stable, Directed Vision during Omnidirectional Locomotion

Samuel Shaw[1], Guillaume Sartoretti[2], Jake Olkin[2], William Paivine[2], and Howie Choset[2]

***Abstract*— In this paper, we focus on the problem of directing the gaze of a vision system mounted to the body of a high-degree-of-freedom (DOF) legged robot for active perception deployments. In particular, we consider the case where the vision system is rigidly attached to the robot's body (i.e., without any additional DOF between the vision system and robot body) and show how the supernumerary DOFs of the robot can be leveraged to allow independent locomotion and gaze control. Specifically, we augment a workspace central pattern generator (CPG) with omnidirectional capabilities by coupling it with a body pose control mechanism. We leverage the smoothing nature of the CPG framework to allow online adaptation of relevant locomotion parameters, and obtain a stable mid-level controller that translates desired gaze orientation and body velocity directly into joint angles. We validate our approach on an 18-DOF hexapod robot, in a series of indoor and outdoor trials, where the robot inspects an environmental feature or follows a pre-planned path relative to a visually-tracked landmark, demonstrating simultaneous locomotion and directed vision.**

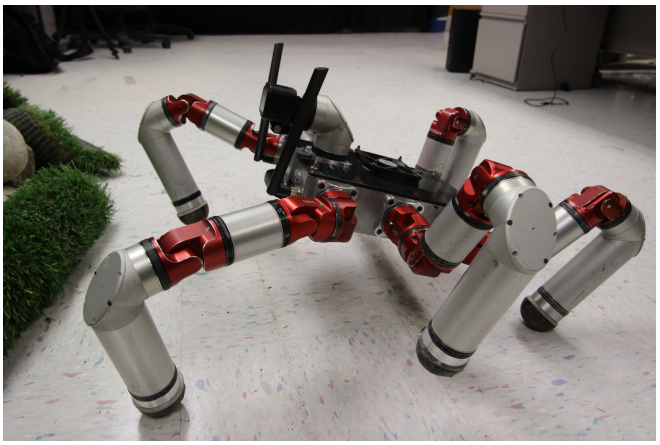

Fig. 1: Hexapod robot adapting its body pose to direct the gaze of a vision system upward. The vision system is rigidly attached to robot's body (i.e., with no additional articulation).

I. Introduction

Active perception for locomoting systems considers the simultaneous problem of robot locomotion and gaze control, usually during autonomous deployments of mobile robots [1], [2]. In this paper, we focus on high-DOF legged robots since they are a versatile platform suitable for traversing unstructured terrains [3], [4], [5], [6], [7]. We consider the case where a vision system is rigidly mounted to the body of a robot (as pictured in Fig. 1), meaning that the direction of the camera's view is fixed to the body's orientation. Our approach leverages a robot's locomotive DOFs to simultaneously transport the robot through its environment and fixate a vision system onto a feature of interest (e.g., for landmark-based localization, mapping, and inspection [8], [9], [10]). We propose a mid-level control mechanism that translates high-level locomotive and gaze commands into robot limb joint angles. The first component of our controller is a workspace CPG [11], [12], [13], [14] that generates foot trajectories for omnidirectional locomotion based on the robot's locomotive goals. The second component of our controller is an $SE(3)$ body pose control mechanism that positions these foot trajectories relative to the robot's body for simultaneously locomotion and body pose control.

CPGs [3], [15], [16], [17], [18] can either be defined in the joint space of the robot (i.e., with outputs directly serving as joint angles, similar to their biological inspiration) or in the workspace (i.e., with outputs describing the position of the robot's feet). Recent works have explored both joint space [19] and workspace [11], [12] CPG-based omnidirectional motion. However, these works assumed planar environments and did not control body pose online for stable locomotion. Workspace CPG approaches presented in other works [13], [14] explored body control via pitch only for stable forward locomotion on inclined slopes.

In this work, we propose a mechanism that controls the full body pose of a legged robot online in parallel to omnidirectional locomotion, in order to direct the gaze of the onboard vision system. Specifically, rotation provided by the pose control mechanism (PCM) directs the gaze of the camera, whereas the translation positions the body's center of mass to stabilize locomotion (e.g., on steep or unstructured terrain). We validate our method experimentally in a number of indoor and outdoor scenarios that demonstrate the locomotive controller's ability to concurrently produce omnidirectional locomotion and stable, directed vision, both on flat and inclined ground. Specifically, in these experiments, the robot locomotes on a path defined relative to a feature of interest while continually directing its gaze toward the feature.

This paper is structured as follows: Section II details the problem considered and introduces key notations. Sections III and IV present our controller's two modules: a PCM for directed vision and workspace CPG for locomotion. Section V experimentally validates our controller. Finally, Section VI summarizes our approach and presents directions for future works.

[1]S. Shaw is with the department of Computer Science at Tufts University, Medford, MA 02155. samuel.shaw@tufts.edu

[2]G. Sartoretti, H. Choset, J. Olkin, and W. Paivine are with the Robotics Institute at Carnegie Mellon University, Pittsburgh, PA 15213, USA. {gsartore,choset}@cs.cmu.edu, {jolkin,wjp}@andrew.cmu.edu

II. Notations and Problem Analysis

In this section, we explain how we develop our control mechanism in the robot's workspace, before we introduce reference frames that allow us to analyze the problems of locomotion and body pose control independently. Then, we analyze the locomotive problem and highlight key considerations for the design of our CPG model. Finally, we describe the body pose control problem and how we implement the controller in a way that is not adversarial to locomotion.

A. Inverse Kinematics Approach

In this work, we consider an articulated, bilateral legged system with a single rigid body, referred to as the robot's *body*, to which all legs are connected. Such a high-DOF legged robot can adapt its configuration to re-orient its body without changing its foot positions in the world. Thus, through careful control, we can leverage these locomotive degrees of freedom to orient the vision system's gaze and position the body's mass in a manner non-adversarial to the foot trajectories generated by the CPG.

Our approach achieves the desired locomotion and body pose by controlling the robot's foot positions relative to its body. Once these foot positions are computed, we obtain joint angles via the robot's inverse kinematics (IK). Therefore, our main quantity of interest is the position of the feet in the body frame, given by $F_B \in \mathbb{R}^{3\times n}$:

$$F_B = \begin{bmatrix} x_1 & \cdots & x_n \\ y_1 & \cdots & y_n \\ z_1 & \cdots & z_n \end{bmatrix}, \tag{1}$$

with n the number of legs on the robot considered.

B. Reference Frames

We first define the *gaze frame*. We align the gaze of the vision system with the y-axis of gaze frame; as such, the orientation of the gaze frame in the world describes the gaze of the vision system. Since the vision system is rigidly mounted to the robot's body, the gaze frame is equivalent to the robot's body frame. Second, we define the *locomotive frame*, in which the workspace CPG develops foot trajectories. We design the workspace CPG such that feet in the stance phase of the gait move in the xy-plane of the locomotive frame. We achieve body pose control by re-positioning and re-orienting the locomotive frame with respect to the body frame. That is, by moving the feet of grounded legs with respect to the body, we position/orient the body in the world.

C. Gaze Control via Body Pose

The PCM regulates the robot body's six degrees of freedom with respect to its grounded feet. Specifically, we use body rotation to direct a rigidly-mounted camera and body translation for body-positioning constraints such as body-height and center-of-mass positioning. To implement the PCM, we observe that applying a rotation/translation matrix directly to F_B results in the inverse rotation/translation of the body in the world, assuming that the robot's feet remain anchored to the ground (no slip).

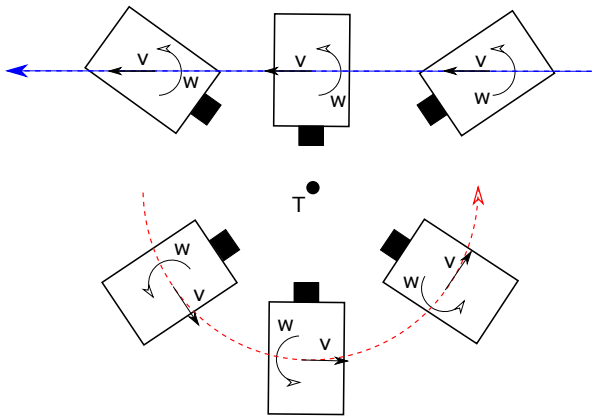

Fig. 2: Top view of planar scenarios that demonstrate the necessity of omnidirectional locomotion. Each scenario features three snapshots of the robot's body orientation through time. These snapshots highlight changes in body orientation; translational velocity, $\vec{v}$; and angular velocity, ω, through time. Top: robot moving linearly relative to a target point of interest, denoted T. Bottom: robot orbiting T. The solid black rectangle at the front of the robot's body represents a vision system directed at T.

We define the homogeneous transform, $G \in SE(3)$, referred to as the *ground transform*, which describes the locomotive frame with respect to the body frame. That is, in particular, G^{-1} describes the pose of the robot's body with respect to the ground. The PCM achieves the correct body pose by adapting G based on sensory feedback (e.g., IMU data) to position the foot trajectories with respect to the body and achieve the desired body pose during locomotion. Note that, since the homogeneous transform G only applies a translation and/or rotation, it preserves the spatial relationships between foot positions. Preserving these spatial relationships is essential in ensuring that locomotion occurs as expected.

D. Gaze Control via Omnidirectional Locomotion

We rely on explicit control of the robot's linear and angular velocity (yaw) to allow the robot to keep its gaze *vertically* aligned with a feature of interest while locomoting on a path relative it. As illustrated by Fig. 2, even paths that characterize simple inspections regularly require the robot to move in a direction not aligned with its gaze. In particular, omnidirectional locomotion to supplements the yaw-control provided by the PCM, which is limited by the robot's workspace.

As such, we define the main high-level input variables as follows: ω, the desired angular (yaw) velocity of the robot locomotive frame; and, $\vec{v}$, which defines the desired translational velocity of the robot in the xy-plane of the locomotive frame. We choose $\omega > 0$ to define counter-clockwise rotation.

We translate these body velocities into individual foot trajectories that will collectively achieve the desired translation and rotation of the robot, We consider the problem of omnidirectional motion as one of locomoting around an axis parallel to the z-axis of the locomotive frame; we define a point $T = (T_x, T_y, 0)$ in the locomotive frame through which

this axis passes. Based on the magnitudes of $\vec{v}$ and ω, we compute the rotation radius, r_0:

$$r_0 = \begin{cases} \frac{|\vec{v}|}{\omega}, & \omega \neq 0 \\ \infty, & \omega = 0. \end{cases} \tag{2}$$

To achieve pure rotation, T is placed at the origin of the locomotive frame with $r_0 = 0$. Conversely, to achieve pure translation, T must be placed at infinity. A placement of T that results in an intermediate value of r_0, as shown in Fig. 3, will provide a composition of translation and rotation (movement along an arc of a circle). Changing T through time allows for the traversal of a path of arbitrary shape.

We set the x- and y-component of T:

$$\begin{cases} T_x = r_0 \cos(\frac{\pi}{2} + \arctan(\frac{v_y}{v_x})) \\ T_y = r_0 \sin(\frac{\pi}{2} + \arctan(\frac{v_y}{v_x})), \end{cases} \tag{3}$$

which places T at a distance of r_0 from the origin of the locomotive frame, at a position to command the robot to translate with velocity $\vec{v}$ and rotate with speed ω.

Given the position of T, it is now possible to compute a foot's average *stance speed*, $\bar{v}_{s_i}$, which is the average speed at which a grounded foot must move relative to the robot's body. Each foot trajectory will be developed as a rhythmic motion relative to an independent origin point in the locomotive frame. We let the columns of $C \in \mathbb{R}^{3\times n}$ be these leg-by-leg origins in the locomotive frame:

$$C = \begin{bmatrix} x_1 & \cdots & x_n \\ y_1 & \cdots & y_n \\ 0 & \cdots & 0 \end{bmatrix}. \tag{4}$$

A foot's average stance speed is directly proportional to the distance between the foot trajectory origin given by C and the robot's center of rotation, T.

We let $r \in \mathbb{R}^{1\times n}$ define the distance between the point of rotation, T, and the foot trajectory origin:

$$r_i = \sqrt{(C_{1,j} - T_x)^2 + (C_{2,j} - T_y)^2}. \tag{5}$$

If a rotation is to occur ($\omega \neq 0$), legs which are farther from the point of rotation must contribute a larger average speed than legs which are closer. Thus, the average stance speed is defined in terms of the magnitude of ω and r_i:

$$\bar{v}_{s_i} = r_i \cdot |\omega|. \tag{6}$$

III. Body Pose Control

In this work, we adapt the robot's body pose in the world to perform two goals. First, the control of the body's orientation directs the gaze of the on-board vision system. Second, the control of the body's translation centers the body's mass within the support polygon formed by its feet for stable locomotion.

A. Computing Body Pose Correction

The homogeneous transform G positions the robot's foot trajectories in the body frame. We assume that the robot's feet in the stance phase of the gait remain grounded with little slippage. Therefore, movement of the robot's stance feet relative to the body will in turn move the robot's body in the world. Thus, we define $D \in SE(3)$ as the desired

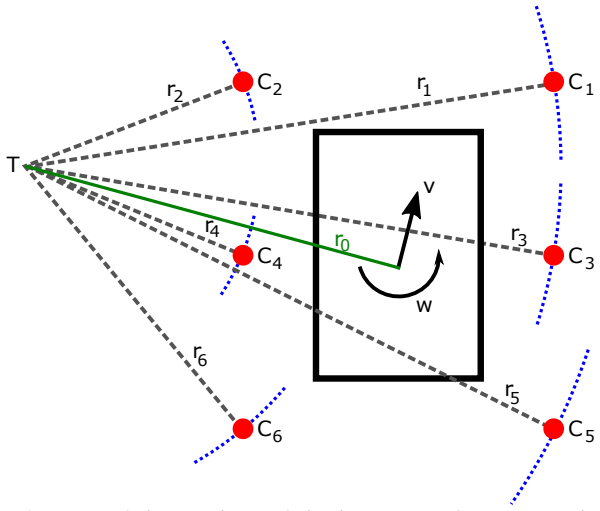

Fig. 3: View of the xy-plane of the locomotive frame. To achieve a planar velocity, $\vec{v}$, and planar angular velocity, ω, we consider locomotion around avertical axis positioned at T. The red circles and black rectangle represent the robot's feet and body respectively, and the blue dotted lines the feet's trajectories on the ground.

homogeneous transform relating the locomotive frame to the body – a target value for G.

We adjust the yaw of the vision system's gaze exclusively through locomotion and the roll and pitch through the body pose controller. Therefore, we design the rotation component of D ($D_{SO(3)}$) to be yaw-free such that $D_{SO(3)}$ controls only the roll and pitch of the gaze. To develop a yaw-free D, we must remove any yaw-rotation with respect to the y-axis in the world frame. To this end, for a given transform, $S \in SO(3)$, we first look for the normalized, planar vector in the world's xy-plane:

$$z_y = \frac{\begin{pmatrix} -i & 1 & 0 \end{pmatrix} \cdot \left(S \cdot \begin{pmatrix} 0 & 1 & 0 \end{pmatrix}^T \right)}{\left\| \begin{pmatrix} -i & 1 & 0 \end{pmatrix} \cdot \left(S \cdot \begin{pmatrix} 0 & 1 & 0 \end{pmatrix}^T \right) \right\|_2} = e^{i\,\theta_S}. \tag{7}$$

Then, from the yaw angle θ_S of S with respect to the y-axis of the world frame, we can express the yaw-component of the transform S as $R_z(\theta_S)$ with:

$$R_z(\theta_S) = \begin{bmatrix} \cos(\theta_S) & -\sin(\theta_S) & 0 \\ \sin(\theta_S) & \cos(\theta_S) & 0 \\ 0 & 0 & 1 \end{bmatrix} \in SO(3). \tag{8}$$

Toward designing $D_{SO(3)}$, we define $B \in SO(3)$ to be the desired body orientation in the world frame. Note that ultimately all yaw-components will be removed; this means that B transforms differing only in yaw will result in the same robot behavior. Additionally, B is terrain-independent; for example, regardless of G, $B = \mathbb{I}_3 \in SO(3)$ always corresponds to a level body with respect to the world. Using B, we define $\tilde{B} \in SO(3)$ to be the transform relating the current body orientation in the world frame, given by $P \in SO(3)$, to the target body orientation, B:

$$\tilde{B} = B \cdot P^{-1}. \tag{9}$$

We design $D_{SO(3)}$ to adapt the body's roll and pitch while preserving its heading to ensure that we can stabilize a rigidly attached vision system without introducing unwanted

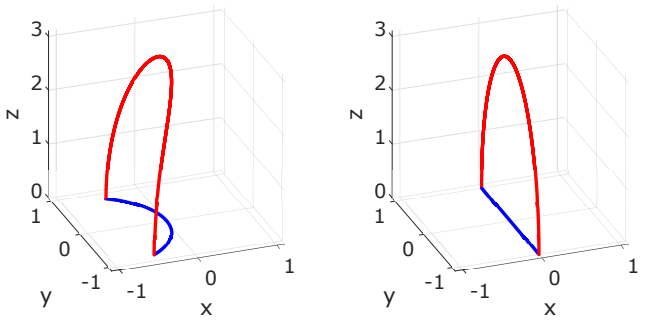

Fig. 4: View of the trajectory produced by the cylindrical CPG for the i^{th} foot relative to the position given by the i^{th} column of C in the locomotive frame. The stance phase is shown in blue in the xy-plane, and the flight phase in red. Here, the stride length and the step height kept constant, while only the curvature of the trajectory $\frac{1}{r_i}$ is varied (left: $r_i = 1$, right: $r_i = 1000$).

yaw rotations. Thus we build $D_{SO(3)}$ by removing the yaw-component of $\tilde{B}^{-1}$:

$$D_{SO(3)} = G_{SO(3)} \cdot \overbrace{R_z(\theta_{\tilde{B}^{-1}})^{-1} \cdot \tilde{B}^{-1}}^{\textit{yaw-free } \tilde{B}^{-1}}. \tag{10}$$

We design the translation component of D ($D_{\mathbb{R}^3}$) such that the body center remains vertically centered (with respect to the world) within the robot's support polygon. This body positioning ensures stable locomotion even on steep terrain. We write $D_{\mathbb{R}^3}$ as:

$$D_{\mathbb{R}^3} = \overbrace{p}^{\textit{nominal translation}} + \overbrace{L \cdot (L^{-1} \cdot p - p)}^{\textit{stability translation}}, \tag{11}$$

with $L = G_{SO(3)} \cdot P \cdot R_z(\theta_P)^{-1} \in SO(3)$ and $p = [0, 0, h]^T$, where $h \in \mathbb{R}$ is a negative value defining the body height. With the rotation and translation components computed in Eq.(10) and Eq.(11), we assemble D as follows:

$$D = \begin{bmatrix} D_{SO(3)} & D_{\mathbb{R}^3} \\ 0^{1\times 3} & 1 \end{bmatrix}. \tag{12}$$

B. Incremental Ground Transform Updates

We let the homogeneous transform $R \in SE(3)$ correct G toward its desired value, D:

$$R = G^{-1} \cdot D. \tag{13}$$

We want to update G in a manner that will result in smooth body motion; updating G based on R in a single timestep would result in a large, quick body motion, not suitable for vision or stable locomotion. Therefore, we define $\tilde{R} \in SE(3)$ as an increment of R, composed from a fraction of the corrective rotation and translation given by the homogeneous transform R. Toward computing $\tilde{R}$, we decompose the rotation component of R into a rotation axis, $\hat{n}_R \in \mathbb{R}^3$, and rotation angle, $\theta_R \in \mathbb{R}$, and we extract the translation component, $e_R \in \mathbb{R}^3$. We then use these three components to build $\tilde{R} \in SE(3)$, an increment of R: $\hat{n}_{\tilde{R}} = \hat{n}_R$, $\theta_{\tilde{R}} = \alpha \cdot \theta_R$, and $e_{\tilde{R}} = \beta \cdot e_R$, where $\alpha \in \mathbb{R}$ and $\beta \in \mathbb{R}$ govern the rotation and translation step size, respectively. To take a step toward the desired body pose, we update G using $\tilde{R}$:

$$G \leftarrow \tilde{R} \cdot G. \tag{14}$$

C. Positioning Locomotive Outputs

We achieve the desired body pose by applying the transform G to the foot positions generated by the CPG in the locomotive frame to move these positions into the body frame. To do so, we define $F_L \in \mathbb{R}^{3\times n}$ to be the robot's foot positions generated by the CPG in the locomotive frame:

$$F_L = \begin{bmatrix} x_1 & \cdots & x_n \\ y_1 & \cdots & y_n \\ z_1 & \cdots & z_n \end{bmatrix}. \tag{15}$$

By applying G, we obtain F_B as given in Eq.(16), the foot positions in the body frame:

$$\begin{bmatrix} F_B \\ 1^{1\times n} \end{bmatrix} = G \cdot \begin{bmatrix} F_L \\ 1^{1\times n} \end{bmatrix}. \tag{16}$$

IV. Cylindrical Workspace CPG

To achieve explicit control of the robot's linear and angular velocities, we consider a workspace CPG expressed in cylindrical coordinates extending [3], [17]:

$$\begin{cases} \dot{\theta}_i(t) = \gamma(1 - H_i(\theta_i(t), z_i(t)) \cdot \theta_i(t) - (2\pi f)\frac{a}{b} \cdot z_i(t) \\ \dot{z}_i(t) = \gamma(1 - H_i(\theta_i(t), z_i(t)) \cdot z_i(t) + (2\pi f)\frac{b}{a} \cdot \theta_i(t) \\ \qquad +\lambda \sum K_{ij} z_j, \end{cases} \tag{17}$$

where $f \in \mathbb{R}$ defines the frequency of the gait cycle, $\gamma \in \mathbb{R}$ defines the forcing to the limit cycle, $\lambda \in \mathbb{R}$ defines the coupling strength, H defines the shape of the limit cycle, and $K \in \mathbb{R}^{n\times n}$, the coupling matrix [3], [17], defines the gait by setting the phase relationship between legs.

Since our analysis characterizes omnidirectional motion as locomotion around an axis, it is natural to choose a cylindrical coordinate system with origin at T in the locomotive frame, as described in Section II. Relative to this origin, we then write each foot position as $[r_i(t), \theta_i(t), z_i(t)]$. By doing so, we let the r coordinate for each foot directly be r_i given by Eq.(5). Differently, the θ- and z-coordinates of each foot trajectory are controlled by the CPG's oscillators.

As in [3], a Hamiltonian function defines the CPG's limit cycle, i.e., a closed path in the phase space. We choose the following function to obtain an elliptical limit cycle:

$$H_i(\theta, z) = \frac{\theta^2}{a^2} + \frac{z^2}{b^2}, \tag{18}$$

where $a \in \mathbb{R}$ defines one-half the arc of a step in radians and $b \in \mathbb{R}$ defines the maximum step height in cm. In particular, a_i is set as:

$$a_i = \frac{s_i}{2r_i}, \tag{19}$$

where $s_i \in \mathbb{R}^{1\times n}$ represents the arc-length of the foot trajectory during the stance phase of the gait. Note: s_i is a function of $\bar{v}_{s_i}$ in Eq.(6) and K; we detail this relationship in Section V when we discuss the CPG implementation details. Note that with regard to this update of a_i, the CPG framework presents a key benefit: when a_i is updated with a change of $\vec{v}$ or ω, the dynamical system naturally smoothly converges to its new limit cycle.

We introduce $\phi_i \in \mathbb{R}^{1\times n}$ as a leg-by-leg offset on $\theta(t)$ used to center the i^{th} foot trajectory at the position defined by the i^{th} column of C:

$$\phi_i = \arctan\left(\frac{C_{2,j} - T_y}{C_{1,j} - T_x}\right), \tag{20}$$

with C and T from Eq.(4) and Eq.(3), respectively. Finally,

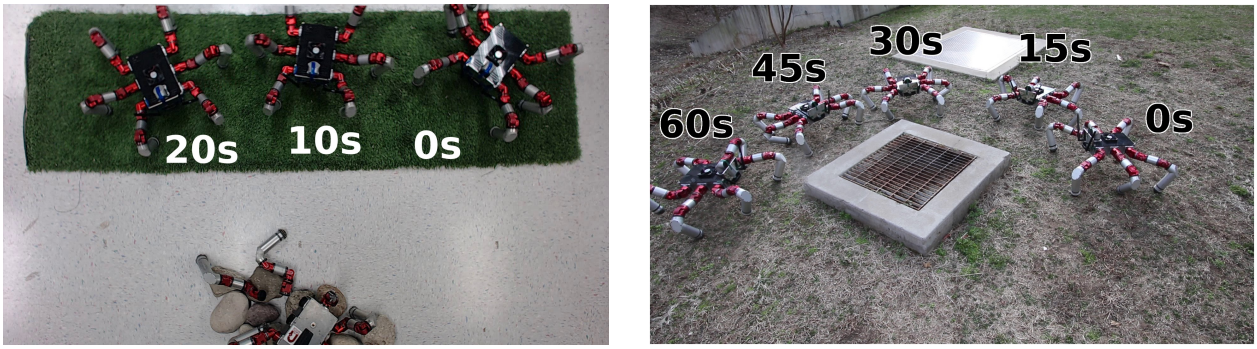

Fig. 5: Experimental validation of the locomotive controller. The body is commanded to be level in the world and at a constant height from the ground. Left: An indoor linear inspection; the robot translates left while keeping its gaze on the environment feature. Right: An outdoor orbital inspection; the robot moves around the environment feature at constant radius while maintaining it in its gaze.

using the CPG outputs we position the feet in the locomotive frame:

$$\begin{cases} F_{L_{1,i}} = -r_i \cdot \cos(\theta_i(t) + \phi_i) - T_x \\ F_{L_{2,i}} = -r_i \cdot \sin(\theta_i(t) + \phi_i) - T_y \\ F_{L_{3,i}} = \max(z_i(t), 0). \end{cases} \tag{21}$$

The z-coordinate is clipped at 0 so that during the stance phase of the gait the foot remains grounded at a constant height (within the xy-plane of the locomotive frame). This limit cycle clipping is demonstrated visually in Fig. 4.

V. Experimental Validation

In this section, we discuss a number of important considerations for implementing this controller on hardware. We begin by describing the configuration of the robot we use, before detailing our CPG parameter choices. Finally, we present the results of our implementation through a series of hardware experiments.

A. Robot Description

To validate our approach, we performed hardware experiments using an 18-degree-of-freedom hexapod robot. The robot features a versatile mounting point on the front of the body, which allows for the attachment of a camera. The joint-modules themselves fully provide the robot's on-board sensing capabilities; each contains an inertial measurement unit (IMU) and encoders [20].

B. CPG Implementation Details

1) Gait-Specific Considerations: We choose the alternating tripod gait for our implementation for its static stability. We implement the alternating tripod gait in the CPG framework using the coupling matrix, K:

$$K = \begin{bmatrix} 0 & -1 & -1 & 1 & 1 & -1 \\ -1 & 0 & 1 & -1 & -1 & 1 \\ -1 & 1 & 0 & -1 & -1 & 1 \\ 1 & -1 & -1 & 0 & 1 & -1 \\ 1 & -1 & -1 & 1 & 0 & -1 \\ -1 & 1 & 1 & -1 & -1 & 0 \end{bmatrix}. \tag{22}$$

The alternating tripod gait considers two groups of legs, where each group operates in the stance phase for one-half of the gait cycle with no overlap of the other group's stance phase. With knowledge of the gait's characteristics, we can compute the average speed a leg must attain throughout the gait cycle, $\bar{v}_i$. For the alternating tripod gait, we set $\bar{v}_i$:

$$\bar{v}_i = \frac{\bar{v}_{s_i}}{2}, \tag{23}$$

where $\bar{v}_{s_i}$ is the average speed of a leg during the stance phase as given by Eq.(6).

We cannot handle changes in $\bar{v}_i$ by adapting the gait cycle frequency, f, on a leg-by-leg basis without disturbing the phase relationships defined by the coupling matrix. Instead, we compute a suitable f for all legs and then adapt s_i on a leg-by-leg basis to achieve the desired foot velocities.

The step frequency is set such that the leg that must attain the highest average velocity must step with the maximum step length, defined by s_m. Then, given a suitable step frequency suitable for all legs, we compute each foot's stride length based on the average speed it must operate at. We determine a suitable step frequency and foot-specific stride length:

$$f = \frac{\omega}{|\omega|} \cdot \max_i\left(\frac{\bar{v}_i}{s_m}\right) \quad s_i = \frac{\bar{v}_i}{|f|}\ , \tag{24}$$

where we define $\bar{v}_i$ as in Eq.(23).

2) Numerical Considerations: During implementation, certain modifications must be made to the CPG model outlined in Section IV due to numerical considerations. In our implementation, we set the minimum limit to be $\omega = 0.0001$, which eliminates almost all rotation, but places a finite limit on r_0. To keep the CPG stable even when the center of rotation is far from the robot and r_0 is large, the θ values of the CPG are scaled by a factor of $r_0 + 1$. Specifically, in practice, we rewrite Eq.(19) to read:

$$a_i = \frac{s_i}{2r_i}(r_0 + 1). \tag{25}$$

Note that the $\theta_i(t)$ will then also be scaled up, and need to be rescaled by $\frac{1}{r_0+1}$ in Eq.(21).

C. Open-loop Locomotion

We devised inspection trials to experimentally validate the locomotive controller's omnidirectional capability. In these trials, we define a path in the target frame by providing time-dependent $\vec{v}$ and ω commands and the initial position of the robot. Additionally, no visual feedback of any kind is used to localize the robot in its environment. The environment the robot traverses is level, and we command the robot's body to be level with respect to the ground (resulting in

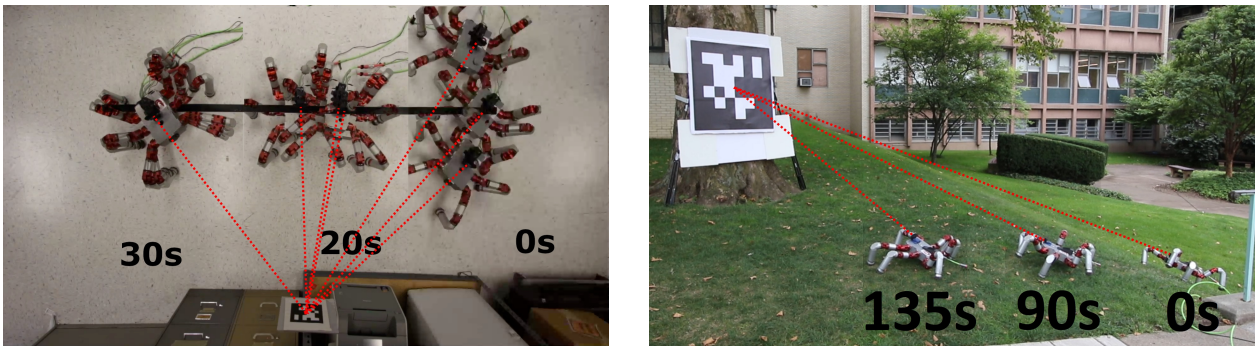

Fig. 6: Closed loop experiments with visual feedback. The robot localizes itself relative to the AprilTag, and adapts its linear and angular velocities $\vec{v}$ and ω to remain on a linear path; the robot also adapts its body pose to keep the AprilTag in frame of the onboard vision system. Snapshots demonstrate the robot's progress over time. Left: An indoor trial where the robot is started at three different initial positions at $t = 0$s, before converging to and progressing along the same path (black solid line). Right: An outdoor trial where the robot starts on a 25-degree incline, before climbing the slope and continuing on flat ground. We leverage the translation component of our body pose control mechanism to center the robot's body within its support polygon to remain stable while climbing the slope.

$G_{SO(3)} = \mathbb{I}_3 \in SO(3)$). In an indoor trial, the robot moves linearly with respect to a feature of interest; to do so, we vary the direction of $\vec{v}$ and the magnitude of ω with time, respectively. Specifically, we set:

$$\vec{v}(t) = \begin{bmatrix} |\vec{v}|\cos(\eta(t)) \\ |\vec{v}|\sin(\eta(t)) \end{bmatrix} \quad w(t) = \frac{y_0|\vec{v}|}{r^2+(x_0-|\vec{v}|t)^2}, \tag{26}$$

where $\eta(t) = \arctan(\frac{y_0}{x_0-|\vec{v}|t})$ and $x_0, y_0, \eta(0) = \arctan(\frac{y_0}{x_0}) \in \mathbb{R}$ define the initial position and orientation of the robot in the target frame. In an outdoor trial, the robot orbits a feature of interest, remaining at a constant distance; here, both $\vec{v}$ and ω are constants. Even without any form of feedback, the robot exhibits the desired behavior during the trials as illustrated in Fig. 5. Locomotive performance during these open-loop experiments depends largely on the quality of the ground contacts (foot traction); for the indoor experiments, a strip of artificial turf is used to improve ground traction and increase the consistency of trials. Videos of all trials are available online at `https://goo.gl/jP5TnL`.

D. Vision-Based Path Following

Additionally, we performed experiments to demonstrate the effectiveness of the controller in active perception situations. In these experiments, an AprilTag [21] fixed above the robot served as a feature of interest, used for localization. The robot used visual feedback to adapt PCM and CPG parameters online. Specifically, we adapted the robot's body pitch based on the feature's vertical position in the robot's gaze, we adapted the robot's body roll such that the feature was level in the gaze, and we adapted $\vec{v}$ and ω based on the robot's position relative to the feature to stay on path. With visual feedback included, trials become very robust and repeatable; as illustrated in the left of Fig. 6, during our indoor trials, we intentionally started the robot off its desired path. Here, we demonstrate that with the help of visual feedback, the robot successfully navigates to its desired path and follows it for the remainder of the trial. Additionally, as demonstrated in the right of Fig. 6, in our outdoor trial we tasked the robot with climbing a 25-degree slope before continuing to locomote on flat ground. The body orientation is controlled to keep the feature in-frame and level, and to ensure stable locomotion while climbing the slope, we translate the body based on the sensed ground orientation using Eq.(11). Visual feedback ensures that the control is robust even in the presence of variable terrain – loose dirt, slippery grass, etc. Videos of all trials are available online at `https://goo.gl/jP5TnL`.

VI. Conclusion

In this work, we considered the specific active perception problem where a vision system is rigidly attached to the body of a high-DOF legged mobile robot. To address this problem, we proposed to leverage the robot's supernumerary locomotive DOFs to control its body pose independently from locomotion, as a means to direct the gaze of the on-board vision system. That is, we presented a mid-level controller that decouples a legged robot's locomotion and body pose, by translating high-level body velocity and posture input directly into joint angles. This controller is composed of a CPG that develops foot trajectories and a body PCM that positions those trajectories. By expressing the CPG as a set of coupled dynamical systems, we leverage the smoothing nature of the oscillators to allow online adaptation of the relevant locomotion and posture variables. We finally validated our approach on a hexapod robot in a series of indoor and outdoor visual inspection and trajectory tracking experiments. Although our trials were successful, a limitation of this approach is that it is difficult to determine the feasibility of a velocity and pose command without detailed analysis of the robot's kinematics.

In future works, we would like to rely on this approach to start reasoning about online gaze control in unknown environments. We believe that our approach can serve as a strong foundation to start investigating methods for a robot to simultaneously exploit the current landmark of interest for relative localization, as well as explore its surroundings to uncover other landmarks that it may need to transition its gaze towards in the near future.

ACKNOWLEDGMENTS

This work was supported by NSF grant 1704256.

REFERENCES

[1] R. Bajcsy, "Active perception," *Proceedings of the IEEE*, vol. 76, no. 8, pp. 966–1005, 1988.

[2] S. Soatto, "Steps towards a theory of visual information: Active perception, signal-to-symbol conversion and the interplay between sensing and control," *arXiv preprint arXiv:1110.2053*, 2011.

[3] G. Sartoretti, S. Shaw, K. Lam, N. Fan, M. Travers, and H. Choset, "Central pattern generator with inertial feedback for stable locomotion and climbing in unstructured terrain," in *ICRA 2018 - IEEE International Conference on Robotics and Automation*, 2018, pp. 5769–5775.

[4] M. Bjelonic, N. Kottege, and P. Beckerle, "Proprioceptive control of an over-actuated hexapod robot in unstructured terrain," in *Intelligent Robots and Systems (IROS), 2016 IEEE/RSJ International Conference on*. IEEE, 2016, pp. 2042–2049.

[5] I. Roditis, T. Nitsos, A. Porichis, P. Chatzakos, G. Bertos, K. Lika, and E. Papadopoulos, "Maintaining static stability and continuous motion in rough terrain hexapod locomotion without terrain mapping," in *2016 24th Mediterranean Conference on Control and Automation (MED)*, June 2016, pp. 545–550.

[6] A. Roennau, G. Heppner, M. Nowicki, J. M. Zöllner, and R. Dillmann, "Reactive posture behaviors for stable legged locomotion over steep inclines and large obstacles," in *Intelligent Robots and Systems (IROS 2014), 2014 IEEE/RSJ International Conference on*. IEEE, 2014, pp. 4888–4894.

[7] D. Belter, P. Łabęcki, and P. Skrzypczyński, "Map-based adaptive foothold planning for unstructured terrain walking," in *Robotics and Automation (ICRA), 2010 IEEE International Conference on*. IEEE, 2010, pp. 5256–5261.

[8] G. Costante, C. Forster, J. Delmerico, P. Valigi, and D. Scaramuzza, "Perception-aware path planning," *arXiv preprint arXiv:1605.04151*, 2016.

[9] L. J. Manso, P. Bustos, P. Bachiller, and P. Núñez, "A perception-aware architecture for autonomous robots," *International Journal of Advanced Robotic Systems*, vol. 12, no. 12, p. 174, 2015.

[10] B. Ichter, B. Landry, E. Schmerling, and M. Pavone, "Robust motion planning via perception-aware multiobjective search on gpus," *arXiv preprint arXiv:1705.02408*, 2017.

[11] M. J. Kuhlman, J. Hays, D. Sofge, and S. K. Gupta, "Central pattern generator based omnidirectional locomotion for quadrupedal robotics," Naval Research Lab Washington DC Navy Center for Applied Research in Artificial Intelligence, Tech. Rep., 2014.

[12] V. Barasuol, V. J. De Negri, and E. R. De Pieri, "WCPG: A central pattern generator for legged robots based on workspace intentions," in *ASME 2011 Dynamic Systems and Control Conference and Bath/ASME Symposium on Fluid Power and Motion Control*. American Society of Mechanical Engineers, 2011, pp. 111–114.

[13] C. Liu, Q. Chen, and D. Wang, "CPG-inspired workspace trajectory generation and adaptive locomotion control for quadruped robots," *IEEE Transactions on Systems, Man, and Cybernetics, Part B (Cybernetics)*, vol. 41, no. 3, pp. 867–880, 2011.

[14] C. Liu, D. Wang, and Q. Chen, "Central pattern generator inspired control for adaptive walking of biped robots," *IEEE Transactions on Systems, Man, and Cybernetics: Systems*, vol. 43, no. 5, pp. 1206–1215, 2013.

[15] P. Holmes, R. J. Full, D. Koditschek, and J. Guckenheimer, "The dynamics of legged locomotion: Models, analyses, and challenges," *Siam Review*, vol. 48, no. 2, pp. 207–304, 2006.

[16] S. Rossignol, R. Dubuc, and J.-P. Gossard, "Dynamic sensorimotor interactions in locomotion," *Physiological reviews*, vol. 86, no. 1, pp. 89–154, 2006.

[17] L. Righetti and A. J. Ijspeert, "Pattern generators with sensory feedback for the control of quadruped locomotion," in *Robotics and Automation, 2008. ICRA 2008. IEEE International Conference on*. IEEE, 2008, pp. 819–824.

[18] A. J. Ijspeert, "Central pattern generators for locomotion control in animals and robots: a review," *Neural networks*, vol. 21, no. 4, pp. 642–653, 2008.

[19] C. P. Santos and V. Matos, "CPG modulation for navigation and omnidirectional quadruped locomotion," *Robotics and Autonomous Systems*, vol. 60, no. 6, pp. 912–927, 2012.

[20] D. Rollinson, S. Ford, B. Brown, and H. Choset, "Design and modeling of a series elastic element for snake robots," in *Proceedings of ASME Dynamic Systems and Control Conference (DSCC)*, 2013, pp. V001T08A002–V001T08A002.

[21] E. Olson, "Apriltag: A robust and flexible visual fiducial system," in *Robotics and Automation (ICRA), 2011 IEEE International Conference on*. IEEE, 2011, pp. 3400–3407.